Structure learning in highly redundant motor tasks

CoMPLEX Summer Project, August 27, 2014

Author:

Talfan Evans

Supervisors:

Joern Diedrichsen and Maneesh Sahani

Abstract

The current study investigates structure learning of highly redundant motor tasks. In these tasks, the dimensionality of the control signal exceeds that of the output, such that an infinite number of valid control strategies exist. During learning, the motor system selects strategies based on the optimisation of particular neural and physiological costs. The current study proposes that optimisation occurs respective to a cost based on the statistics of natural movements, and the hypothesis is investigated through an experimental paradigm whereby subjects were required to learn to control a 2-D on-screen cursor through the use of a data glove, which recorded the subjects' hand movements.

Contents

1 Introduction

The natural world is abound with examples of tremendous feats of motor control. One could consider the precise and unwavering motion of a hummingbird, or the grace and coordination of professional sportspersons, to represent the peak of such abilities yet, even the most seemingly mundane tasks encountered in everyday life are deceptively complex. Walking requires the harmonius cooperativity of numerous muscle groups, and even the most elementary of manual manipulations, the grasping of a teacup, requires both precise consideration of sensorimotor stimuli from the fingers to avoid crushing or letting slip.

Moreover, we are able to perform these movements with practical pace and accuracy, lifting the teacup slowly so as to sip with ease and without spillages, or walking without tripping over our own feet.

From an engineering perspective, the challenge of reproducing the grace and efficiency of movement innate to all living organisms is complex and multifaceted. Consequently, in most cases even the performance of state-of-the-art robotics pales in comparison to that of a two year old child, even in tasks for which they have been specifically optimized. The sensors in a robot's motors or joints record position and velocity with far greater precision that do the proprioceptive organs of our bodies, and the sensory information is transmitted digitally and far more rapidly than the comparatively sluggish speeds at which signals are conducted along our axons, yet our bodies are able to compensate for these limitations and still consistently outperform their mechanical counterparts.

Effective motor control is not one, but a seamless integration and mastery of many different components. Incorporation of sensory information requires tolerance to noise, both in the sensors and their environment. Control mechanisms also need to be robust to unpredictable changes in this environment, whilst maintaining practical performance.

This particular aspect can be considered a learning problem. Intuitive to most is the idea that with practice comes improvements in performance, yet the mechanisms by which the sensorimotor system is able to integrate this experience are not clear. Error-based learning, in its simplest form, is one intuitive candidate, however even a superficial analysis reveals its limitations.

Error-based learning operates by penalising actions according to their resultant error, such as throwing a dart at a target. If the dart strikes the board to the right of the target, the next throw should be compensated leftward. If the dart misses the board completely, the compensatory response should be greater, appropriate to the magnitude of the error.

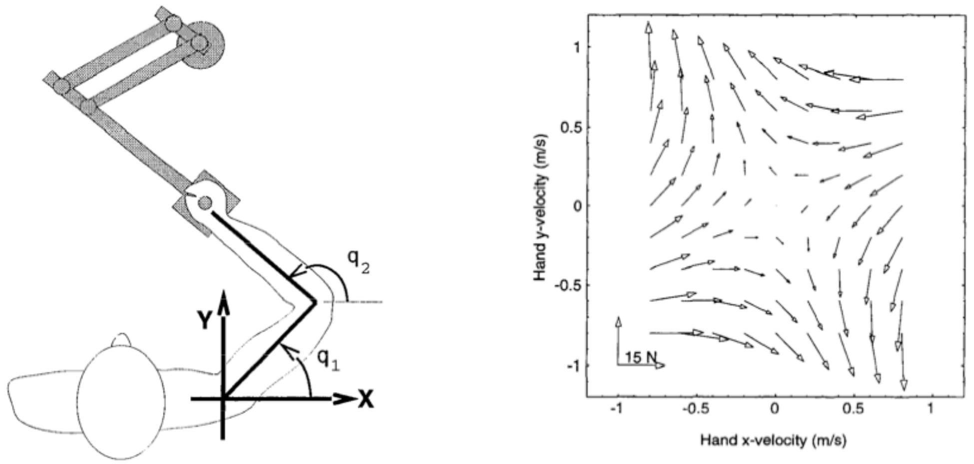

(a) Robotic manipulandum

(b) Velocity-force field

Figure 1

Consider now the problem of maintaining upright an inverted pendulum, achieved by movement of its base to the right of left, where feedback is provided in the form of the pendulum's angle. Designing an error-based algorithm to achieve this task would fail at the first hurdle if the resting position of the pendulum is to hang naturally upside down, as to right it would require movement away from the resting position to generate an initial swing, followed by a sudden reversal in direction to swing past the lowest point so as to swing back up in the other direction, a movement that would require the controller to temporarily increase the angular deviation from the desired upright point. Other standalone mechanisms suffer their own drawbacks, a prominent problem being that of how to compensate for incorrect feedback and misleading environmental variation, emphasizing that a practical solution must incorporate many adaptive responses.

1.1 Towards human-machine interfaces

Though current robotics design does not incorporate a great many principles gleaned from discoveries in neuroscience, in facilitating interaction between humans and machines these principles become more relevant. Advancements in medical imaging, though far from comprehensive are improving access to neuronal data allowing for greater breadth and depth of study of the brain, one goal of being the development of real-time, ambulatory translation for the control of rehabilitative prostheses.

Translation of the neural code into movement is, on a fundamental level, a case of forming a functional relationship between the neural and physical domains, an idea that can be extended as a problem of task learning. Simply put, it is the idea that motor learning is not a process in which performance on a particular task is improved, rather a process through which the brain is able to form an internal representation of the task environment. The idea of 'structure learning' of a tasks lends naturally to the possibility of generalization among tasks which share the same structure, and is importantly connected to the question of whether some element of planning occurs in the motor system prior to movement.

Morasso[1] and Soechting and Laquaniti[2] both observed that during simple reaching tasks, the hand follows quasi-rectilinear and bell-shaped spatial and speed profiles respectively. Though the direction of the hand in this manner is smooth, the shoulder, elbow and wrist joint movements contributing to its motion are not, often involving complex reversals in angular velocity.

Morasso and Flash & Hogan[3] suggested that the movement must be a consequence of a pre-planning of the trajectory by the motor system, anticipating the required muscle coordination through learned experience of similar movement. Others suggested the trajectories to be a natural side-effect of dynamic optimization, whereby the motor system compensates to environmental changes in real-time whilst also attempting to minimize some cost, such as as the rate of change of torque[4].

By studying the effect of force perturbation on movement trajectories, Mussa-Ivaldi[5] and Lacker and Dizio[6] attacked this question directly. In their experiments, subjects held a robotic manipulandum (fig. 1a) while attempting to perform reaching tasks. The manipulandum imposed a force on the movement as a function of the angular position and velocities of the hand such as the field shown in fig. 1b, designed such that the trajectories produced by pre-planned movement and dynamic optimization would be systematically different.

Movement perturbed from its original trajectory was found to return to straight motion, contradicting the predictions of optimal control theory, findings that were later echoed by Dingwell et al.[7, 8], whose subjects were also required to perform reaching movements whilst also minimizing the jerk on a handheld mass attached to a spring. Furthermore, transient aftereffects are observed following removal of the perturbations, showing clearly that some pre-emptive compensatory action is occurring, based on learning not only an internal representation of the task dynamics, but also a geometrical representation of its environment.

1.2 Learning an inverse geometric model of space

These findings led Mosier et al.[9] to further explore how this structure is represented internally. In their experiment, subjects were required to control the motion of a cursor on a screen through movement of their hand. Joint movements were captured using a data glove which was worn by the subject and incorporated 22 bending sensors. The joint angles constituting 'articulation space' were then mapped to the 2-D cursor space. The authors chose a simple linear mapping scheme:

$$\mathbf{P} = \begin{bmatrix} x \\ y \end{bmatrix} = \begin{bmatrix} a_{x,1}, a_{x,2} \cdots a_{x,J} \\ a_{y,1}, a_{y,2} \cdots a_{y,J} \end{bmatrix} \begin{bmatrix} h_1, h_2 \cdots h_J \end{bmatrix}^T + \begin{bmatrix} x_0 \\ y_0 \end{bmatrix} \tag{1}$$

$$\mathbf{P} = \mathbf{AH'} - \mathbf{P_0} \tag{2}$$

Where P represents the cursor screen coordinates and $\mathbf{H'}$ the J-dimensional glove-signal vector, where J is the number of joint angles recorded. $\mathbf{A}$ is the hand-cursor mapping matrix and $\mathbf{P_0}$ a constant-offset value to adjust the resting hand position of the subject to the centre of the screen.

However, the mapping can be more neatly described, and conveniently visualized by considering joint movements relative to their resting positions. Since any screen-coordinate offset is equivalent to a constant linear mapping of the resting glove-signal, equation 2 can also be represented by:

$$\mathbf{P} = \mathbf{AH'} - \mathbf{AH_0} = \mathbf{AH} \tag{3}$$

Where $\mathbf{H} = \mathbf{H'} - \mathbf{H_0}$, the normalized resting glove position.

The linear mapping has many features that make it attractive as a paradigm for the study of structure learning in motor tasks. Firstly, it is unlikely that the subject has had previous exposure to a similar task, allowing all subjects to effectively begin from a common baseline. Secondly, the task captures the essence of the problem of redundant control, introduced by a clear dimensional imbalance between the control (J) and output (x,y) degrees of freedom.

The 'inverse problem' as it is sometimes referred to, is an important consideration where learning of motor control tasks is concerned. The problem arises from the fact that where there exists excess degrees of control freedom, there is redundancy in the system, as the output can be achieved through infinitely many unique combinations of input signals.

The task is also a convenient analogue for the problems encountered in the design of HMIs. In the latter however, the dimensionality imbalance arises from interpreting signals from large numbers of neurons to control a comparatively low-dimensional output, such as a wheelchair.

Whilst the task program performs the forward mapping operation $\mathbf{P} = \mathbf{AH'}$, in order to achieve a particular cursor position on screen, the brain must effectively compute the reverse problem. In order to navigate to a particular screen coordinate the brain must deduce the joint configuration necessary, however whereas the former operation has a unique solution, the latter cannot be so easily deduced.

The dimensionality imbalance means that for any cursor coordinate, there are an infinite number of possible joint configurations. Under the linear mapping, the hand-signal space can therefore be considered as consisting of two separate subspaces. The first is the 2D task-space, containing all articulation-space movements that cause motion of the on-screen cursor. Through manipulation of eq. 3, we obtain:

$$\mathbf{H} = \mathbf{A^T} \cdot \left(\mathbf{A}\mathbf{A^T}\right)^{-1} \mathbf{H} \tag{4}$$

$$\mathbf{H_T} = \mathbf{B_{MP}} \cdot \mathbf{H} \tag{5}$$

Where $\mathbf{B_{MP}}$ represents the Moore-Penrose pseudoinverse. Though many possible inverse mappings exist, this holds particular physical significance, representing the minimal Euclidean distance in articulation space necessary to achieve a cursor-space movement.

While movements in task space translate to space movements, the remaining (J-2)D dimensions constitute the null-space $\mathbf{H_N} = \left(\mathbf{I_J} - \mathbf{A}^{+}\mathbf{A}\right)\mathbf{H}$, where $\mathbf{A}^{+} = \mathbf{A}^{T} \cdot \left(\mathbf{A}\mathbf{A}^{T}\right)^{-1}$ is the M-P pseudoinverse of $\mathbf{A}$ and is everywhere orthogonal to $\mathbf{H_T}$. This is equivalent to the kernel of the mapping matrix $\mathbf{A}$, such that:

$$ker\left(\mathbf{A}\right) = \left\{h \in \mathbf{H} : \mathbf{A}\left(h\right) = 0\right\}$$

Null-space movements do no contribute to cursor-space movements, and are therefore redundant to any task in which cursor manipulation is required. The paradigm is best visualized in reduced dimensions, as illustrated in fig. 2, where $\mathbf{H}$ represents a particular point in a reduced 3D articulation-space. In fig. 2a, the task-space is represented by a family of parallel planes, each orthogonal to the $3-2=1D$ null-space line L_P. Movement within each of these planes translates directly into movement in cursor-space.

Line L_P orthogonally intersects each of the planes and represents a fixed position P in cursor-space, thus for any point in cursor-space, there are an infinite number of articulation-space representations. In fig. 2b, a movement to a new point P_B can be achieved in any number of ways, where the null-space component is the projection of the movement along the line L_{P_B}. The movement $\mathbf{H_A} \rightarrow \mathbf{H_B}$ represents the minimum Euclidean distance in articulation-space, corresponding to the M-P pseudoinverse solution, moving along one particular task-plane.

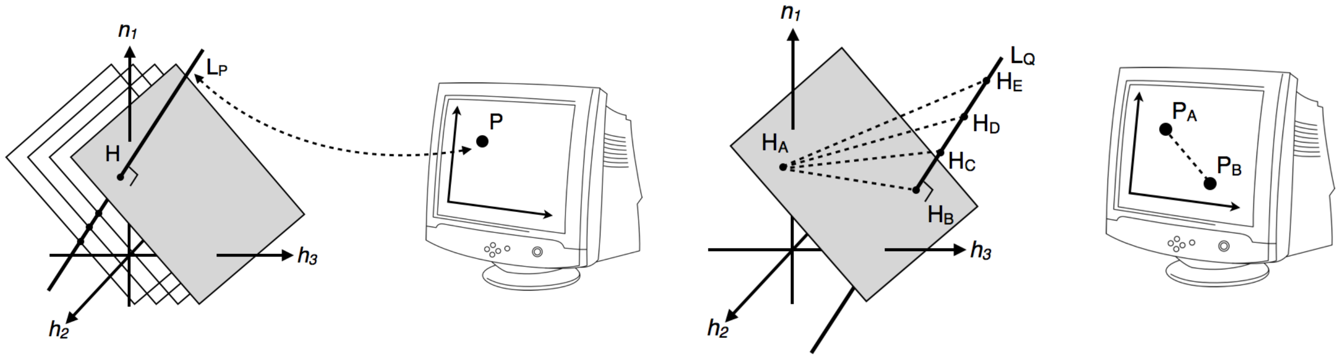

(a) Multiple parallel task-plane projections (b) Null and task-space components

Figure 2

An important prediction of dynamic optimization is that the motor system will 'shift' motor variability to task-redundant dimensions, in order to preserve task-relevant performance. Bernstein[10] was first to publish experimental evidence to support the theory, observing that whilst arm movements and joint angles made during a hammer swinging task varied considerably, the end-point error, here the striking of the nail, was conserved.

The theory has since been reformulated in numerous guises[11], notably by Todorov and Jordan[12] as optimal control theory (OCT), who provide an alternative explanation to the shifting of motor variability framed as the 'minimum intervention principle'. The correction of errors firstly has as associated cost in effort, and secondly may incur unwanted noise in task-relevant space. From an optimal control perspective therefore, there is no incentive to correct null-space variability and all effort is focussed on the task space, leading to an appearance of a 'shift'. Crucially, if subjects were learning an inverse model of the task-space, variability would be expected to reduce equally in both spaces, found to be the case by Mosier et al.

This is however a simplistic interpretation of OCT, as it relies on the assumption that only null-space variability should carry a penalty. However, if there existed constraints, physiological or otherwise between corrections in the task and null-spaces, it is possible that some reduction in null-space would occur as a consequence of reductions in the task-space.

Liu and Scheidt[13] continued investigation into the nature of the inverse structure by testing the effect of visual feedback on learning a similar cursor control task. One group of subjects were required to guide the motion of an invisible cursor to a sequence of targets, marked by a pictorial representation of the required gesture. The subjects rapidly learned to associate positions on the screen with their corresponding hand gestures (translating points in cursor space to points in articulation space), such that even when prompted by blank disks with no pictorial cues, task-error was considerably minimised over initial performance.

However, subjects showed no generalization to new points on the screen, suggesting that no representation of the mapping scheme had been constructed internally. This poor generalization was also observed in subjects provided with a snapshot of the end of trial position of the cursor. A third group, provided with continuous visual feedback showed good generalization to untested target positions, suggesting that gradient feedback is required to effectively explore the task-space structure.

Welch and Bridgemann[14] exposed subjects to alternating trials of prismatic visual displacements. Not only did subjects showed accelerated adaptation rates over the course of the trial, but also performed better than control subjects when generalizing to larger displacements. Braun and Wolpert[15] also showed that increased variability in the task was more beneficial than training on one particular variant. Here, task variation is equivalent to exposing subjects to the wider task structure, again appearing to facilitate greater learning rates.

Liu et al.[16] next experimented with imposing either random visual rotations or scalings on their subjects following an initial common training period. Generalization error during the scaled tasks was found to be better than during rotated ones, and analysis of the Euclidean difference in the estimated inverse mapping B_{est} formed by subjects was significantly higher in the former case. Indeed, the average Euclidean adaptation difference in B_{est} during the scaling tasks was not significant over the difference expected by random noise.

The results suggest strongly that rotations require a reorganization of the internal task-space, prompting subjects to learn a new structure for each rotation. Due to redundancy in the task, these reorganizations lead to the possibility of radically different mapping solutions each time, even in the case of incremental rotations. Conversely, generalization in the scaling tasks only required a re-parameterisation of the original learned structure, giving much more consistent results.

A study conducted by Danziger at al.[17] illustrates this hypothesis more clearly. Subjects were required to guide the motion of a 2 d.o.f robotic arm using a 19-D data glove, given no information about the mapping scheme. At the end of each block, the mapping was updated so as to cancel end-point reaching errors in order to guide subjects' estimation towards the true mapping.

The update was calculated differently for two groups, the first using the analytical M-P solution corresponding to the globally optimal case, and the second using a least mean squares (LMS) gradient descent algorithm, iteratively modifying each component of the mapping matrix until error was minimized below a prescribed threshold. A third group maintained a constant mapping as a control. The M-P inverse group showed no improvement, whilst the LMS-update group consistently outperformed the control group. The observation was attributed to the possibility that whilst LMS finds a locally optimum solution requiring incremental block to block adaptation on the subject's part, the M-P inverse solution was potentially radically different with each iteration, giving subjects' estimation no consistent direction in which to shift.

1.3 Structure exploration

The notion that learning generalizes to tasks of similar structure is an intuitive one. A badminton player would in most cases take to tennis more easily than would a footballer, as would a violin player to the viola over a flautist. Braun and Wolpert [18] frame these as examples of 'paramteric' and 'structural adaptive control' respectively.

The former is fundamentally a question of parameter estimation, where a presupposed task structure is adapted to a similar task. The latter requires learning of a new structure, where interaction between the task d.o.f, its relevant inputs, outputs and their associated ranges and noise must be deduced before paramterisation.

As discussed, deduction of structure in highly redundant control tasks is no trivial matter, and research on explorative strategies is an important subject both for learning theory in general and in engineering contexts.

On a fundamental level, learning a task such as that posed by Mosier et al.[9] is a question of dimensionality estimation and reduction. Where a previous structure is known, exploration of a new task of the same structure would be expected to occur along the originally learned task manifold, in the general case of a non-linear input-output space.

Motor primitives are one theory that have been suggested as a potential strategy employed by the brain to reduce the dimensionality in such tasks, describing the modularization of motor control to functional control units. A functional unit might describe the temporal profile of a particular muscle activity[19], or a predefined coordinated expression within a group of muscles. The total motor output is then the sum of the primitives, weighed by their activity.

A task for which the motor system has many relevant primitives would be easier to learn than a task for which it has none. The location or distribution within the motor system at which primitives are encoded is an open question.

Crucially, motor primitives can aid with dimensionality reduction as each unit encapsulates functional relationships between numerous degrees of freedom within the task, and bear relevance to use-dependent learning where the state of the motor system can change irrespective of the the availability of feedback, such as in the repetition of movements[20, 21].

In this case, the primitives formed would encode information in the form of correlation, biomechanical relationships or neural association, and provide constraints on the form of exploration that can occur within a task. In effect, it can be considered a modularised extension of exploring along a previously learned structure in a task.

1.4 Natural statistics as a basis for structure learning

In learning a novel task such as a hand-to-screen mapping, what exploratory structure should the motor system adopt? Where no previous experience exists, a potential strategy might to be to explore in alignment with modularised structures in the form of motor primitives.

In the context of gesture manipulation in everyday tasks, Ingram and Wolpert[22] introduced the concept of natural statistics. In their study, the authors developed a portable version of the data-glove employed by[9], which was worn by a number of subjects for an extended period during day-to-day activity. The authors used principal components analysis to reduce the dimensionality of the glove data, finding that the first two principal components described over 60.2 +/- 4.1%[22] of the variance in manual activity, and were highly conserved across subjects. The first 10 accounted for 93.5 +/- 1.1%, suggesting that the bulk of day to day activity can be described as a linear combination of comparatively few gestures.

Their work built upon earlier studies, notably by Gentner and Classen[23, 24]. In the first study, the authors used Transcranial Magnetic Stimulation (TMS) of the primary motor cortex to induce random finger movements in subjects. Although there was no geometrical representation between the stimulated region of the brain and the finger movement evoked, there was significant similarity between the variation in TMS-evoked movements and those obtained from observation of the subjects' natural statistics, a finding echoed in later studies by Overduin et al.[25] and presenting clear evidence of hard-wired synergies or motor primitives encoding coordinated muscle activation.

The current study investigates the possibility that exploration of novel task structures is guided by these natural statistics. The experiment first captures the natural statistics of four subjects. The data obtained is subsequently used to predict behaviour in a glove-to-screen cursor manipulation task.

2 Obtaining the natural statistics

In the first part of the experiment, four subjects performed a range of 10 activities for 30 seconds each, emulating the range of movements made in routine everyday tasks. Example activities included typing, using a laptop computer and stacking a set of wooden blocks. Subjects were not informed of the intention of the experiment before hand. Movement in 19 finger joints was continuously recorded by a left-handed Immersion CyberGlove[26], outlined in fig. 3. The raw sensor outputs do not measure finger and thumb abduction relative to an independent coordinate system, rather they measure the relative displacement between neighbouring joints. A calibration procedure was used to map the raw readings to angular measurements. The four distal interphalangeal finger joints (DIPs) and thumb interphalangeal joint were disregarded in order to reduce the dimensionality of the task for future analysis. The decision is justified by the high correlation between the DIPs and IP with their corresponding PIPs and MCP respectively due to biomechanical association, resulting in a reduced 14-D articulation space. The resulting sensor arrangement is detailed in table 1. The abbreviations C, M, P and A refer to CMC, MCP, PIP and abduction angles respectively, and the subscripts t, i, m, r and p refer to the five corresponding hand digits.

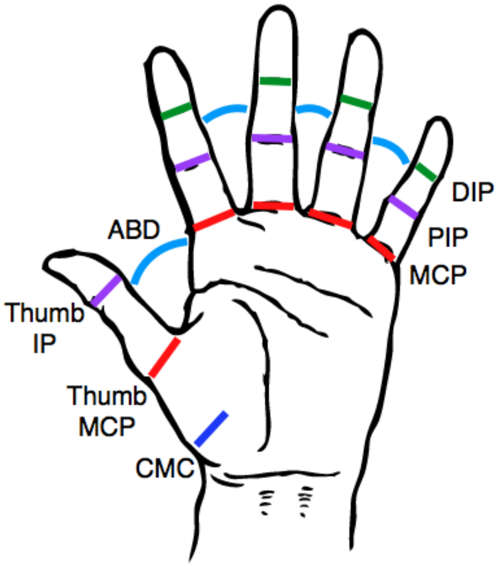

Figure 3: Diagram of glove sensors

No.	1	2	3	4	5	6	7	8	9	10	11	12	13	14
Joint	C_t	M_t	A_{t-i}	M_i	P_i	M_m	P_m	A_{i-m}	M_r	P_r	A_{M-R}	M_p	P_p	A_{r-p}

Table 1: Joint allocations

2.1 Comparing natural statistics

The covariance matrices of the natural statistics obtained for the four subjects is presented in fig. 5. Due to the size of the data files obtained from the experiment, a method was developed (see Appendix) for the modularization, and subsequent combination of covariance matrices in order to reduce the computational load.

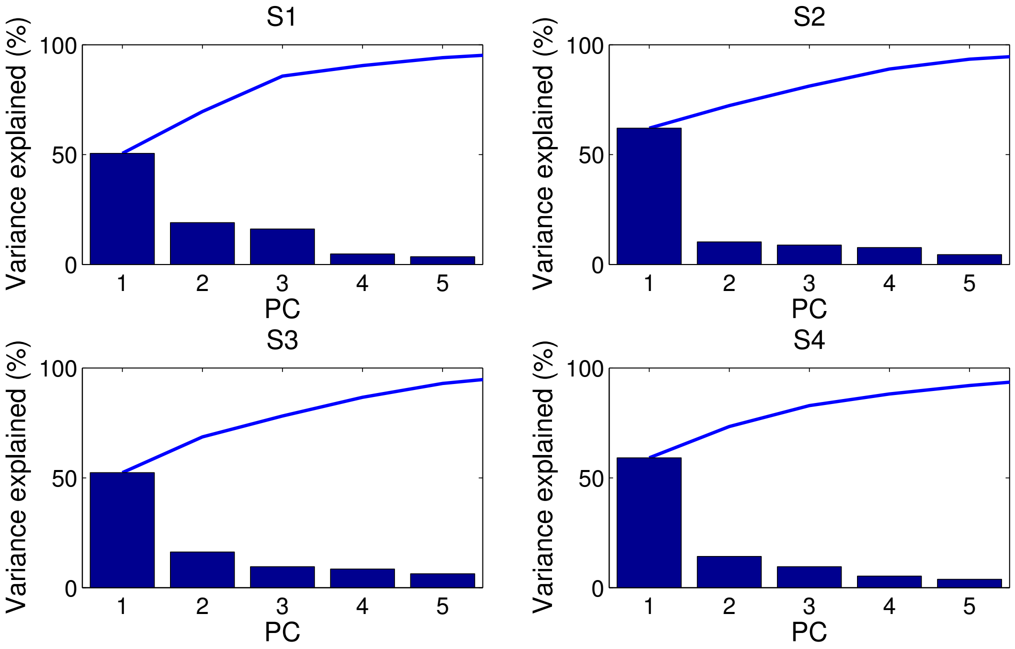

Figure 4: Cumulative variance of the natural statistics

As found by[22], there is high correlation among joints of the same digit, namely the PIPs and MCPs of each. The second highest correlation lies between the middle and index fingers, assumed to arise from the prominence of the key-grip gesture common to many of the tasks.

Movement of the remaining digits is relatively independent, as is abduction. In general, the only significant abduction is between the thumb-index, whereas the interdigit abductions are relatively little used. Interestingly, there is little movement in the thumb MCP, suggesting that most of the movement of the thumb occurs through movement of the CMC.

Bartlett's test[27] was applied, assuming normal distribution of joint angles, showing that the covariance matrices are statistically equivalent ($p<0.01$). A comparison of the cumulative variance explained by descending principal components of the natural statistics is shown in fig. 4. The results show that the first two PCs explain approximately 80-90% of variance, agreeing with findings made by [22] and indicating that the experimental procedure produced a data set representative of the wider study conducted by [22].

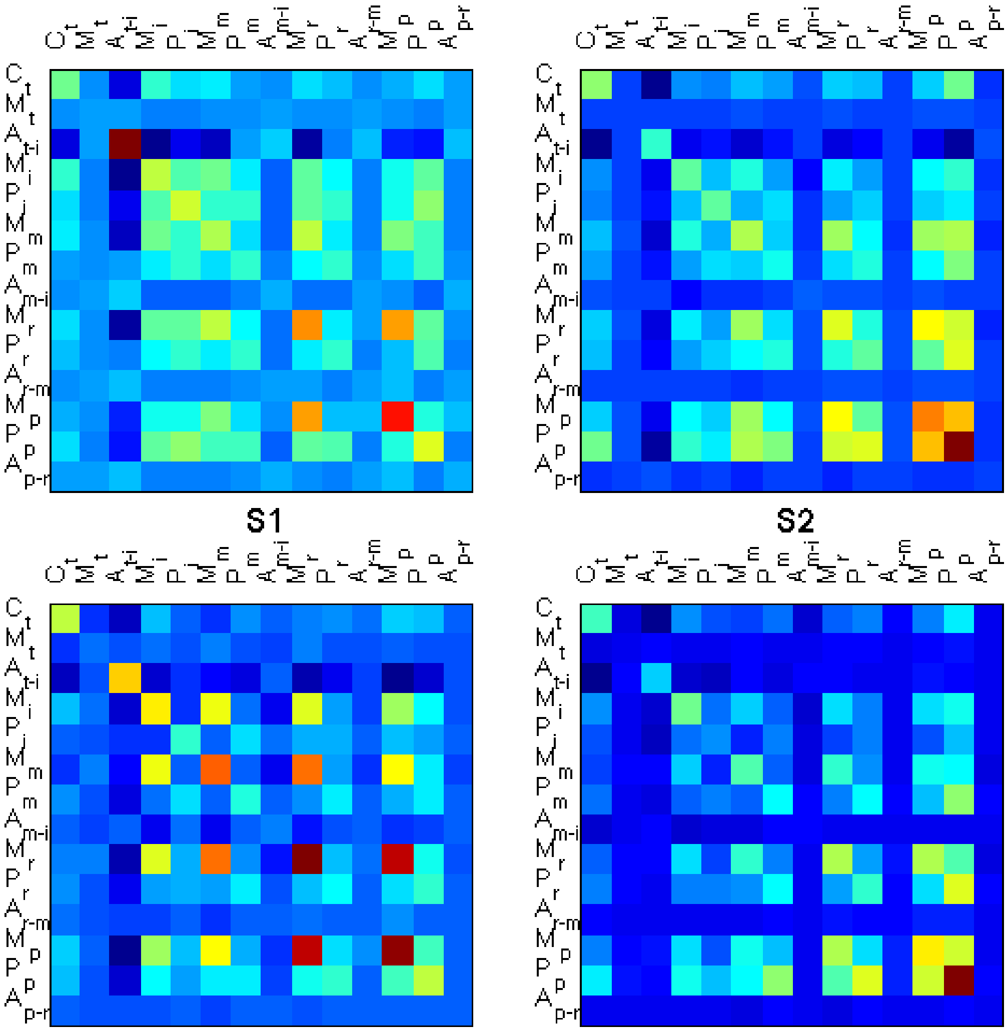

S1 **S2**

S3 **S4**

Figure 5: Covariance matrices of natural statistics

3 Cursor task

The second part of the experiment required subjects to guide a cursor to a number of targets on a computer monitor. Prior to the beginning of each block, subjects assumed a resting hand position, which was approximately constant across subjects and blocks. Though it was not a requirement that the resting position be identical in each block, it was important that it lay in the middle of the range of finger movements to allow subjects to fully exploit the range of the screen.

In each trial, subjects guided the cursor to one of eight targets, spaced at an equal radius in increments of 45 around the centre. The sequence presented to the subjects was coordinated in pseudorandom order such that an equal number of targets appeared in each block. The time to reach each target was not limited, but subjects were encouraged to complete the trials as quickly as possible. The cursor was required to stay in the target position for 10ms, to prevent the subject from 'swiping' through, which would not represent a deliberate strategy. Some end-point error was allowed, giving subjects a small target area of 20 pixels in diameter.

The radius of the targets was set based on previous experimental trial and error, balancing two competing factors. The targets had to be far enough from the centre to elicit purposeful, compound movement of joints from the subject. In a previous trial experiment where the target was set too close, the subject quickly learned to attain the targets through almost singular movement of the thumb and index finger. Whereas this was a clear excercise in efficiently utilizing the task space, the task was effectively reduced in dimensionality to such a degree as to be trivial, not prompting sufficient exploration of the wider task and null-spaces or requiring any significant strategical decisions to be made. Conversely, setting the target too far not only made the task prohibitively difficult, but forced the strategy by making the targets only physiologically attainable by one gesture. The target radius thus had to allow some flexibility over which strategy to adopt to reach the targets whilst providing a reasonable level of challenge. In each experiment, subjects were exposed to two trial variants which took the form:

Centre-out (CO): Subjects were required to return to the centre of the screen after reaching each target, which corresponded to the resting position calibrated at the beginning of the block. Visual feedback was removed upon return to the centre to prevent subjects from conducting unconstrained exploration between trials.

Pinball (PB): Subjects moved continuously between each subsequent target. Continuous visual feedback was provided throughout each trial.

The variants were designed designed to explore firstly whether providing an 'anchoring' resting position at the end of each trial would affect the consistency of the strategies adopted between blocks. Referring to fig. 2b, there are infinitely many valid task-planes along which the motor system could navigate to successfully complete the task. Under the assumption that exploration does not occur perfectly along the initial task-plane, it is reasonable to assume that some drift may occur into the null-space, resulting in strategy shifting between different task-spaces on a trial-to-trial basis. Providing a point of reference at the resting position in the CO trials would possibly mitigate this drift, resulting in a more consistent strategy.

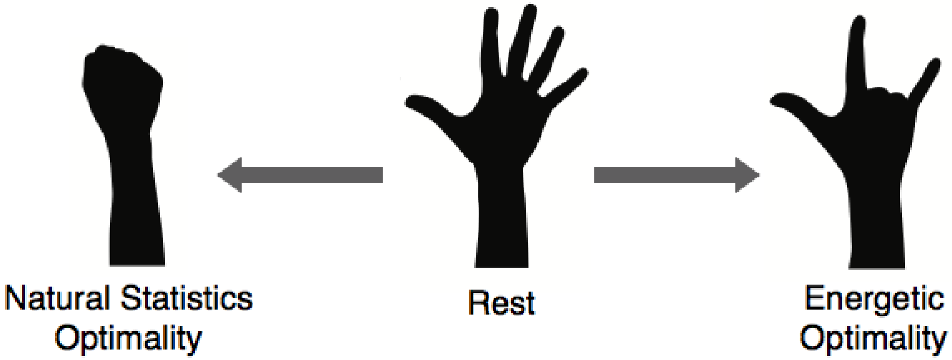

Figure 6: Energetic and natural statistics biased optimality

Secondly, it has been assumed to this point that the motor systems optimal strategy is independent of translation in articulation space. In the centre-out trials, in might be expected that as the subject starts from a constant resting position, the gesture adopted to reach a particular target would, in the case of a well defined strategy, be relatively constant.

Conversely, in the pinball trials the trajectory to a particular target would differ depending on the location of the previous target. In this case, subjects might choose different gestures dependent on optimizing a particular cost function based on the trajectory toward, rather than position of the next target.

For example, consider that to reach a particular target, either of two final gestures is sufficient. The first might correspond to a closed fist; a well-practised and 'comfortable' gesture, and one that would satisfy natural statistics biased optimality. The second sufficient gesture might be a flexed middle and index finger, comparatively infrequently used and not as favourable under natural statistic, but which in biomechanical terms could be argued to be more energetically optimal, as opposed to fully flexing all fingers.

Consider now the situation in fig. 6, where the preceding (resting) gesture is a spread-palm. From this position, the subject could either choose the closed-fist gesture, favourable under natural statistics, or the middle and index flexed gesture, requiring a shorter total distance in articulation space. This choice could be interpreted to discern the internal strategy adopted by the motor system.

The full experiment structure consisted of 8x80 trials blocks of alternating style (4xCO + 4xPB), followed by 4x160 longer length trials (2xCO + 2xCO). Two subjects initiated the experiments with a CO trial, whereas the remaining two started with PB trials.

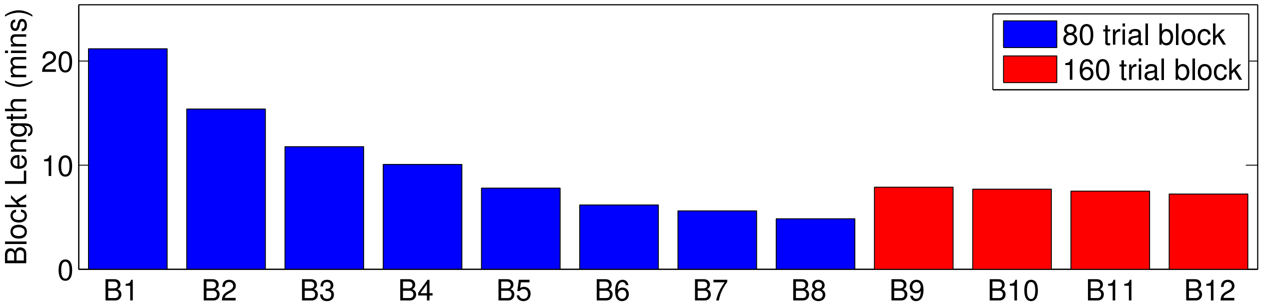

Figure 7: Average block lengths across subjects

The blocks were arranged in this fashion to accommodate the increasing skill of the subjects. On average, subjects required approximately 20 minutes to complete one block of 80 trials, whereas they were able to complete the final block of 160 trials in a much shorter time, illustrated in fig. 7.

The first four blocks constitute the adaptation period, and only the final four blocks are considered in the following analysis, as these are assumed to represent the steady-state strategy aopted by the motor system.

3.1 Defining the mapping matrix

Given the redundancy, novelty and non-intuitive nature of task, for new subjects navigation within cursor-space is unsurprisingly difficult, and here the choice of the forward mapping matrix A is crucial. A randomly generated A would in likelihood lead to a task-space requiring hand gestures that were not only significantly non-intuitive and but also physiologically very demanding and unnatural.

Liu and Scheidt[13] took the first two PCs, producing a $A_{2\times J}$ dimensional matrix that was used as the linear mapping. Physically, this would lead to each point in cursor-space equating to a linear combination of these two PCs, the first PC governing movement in the x and the second in the y direction respectively.

Given the difficulty of the task, a non-intuitive mapping would not be desirable, almost certainly leading to prohibitively long adaptation times. However, introducing an overly-intuitive mapping would possibly lead to a trivial result in which the subjects may consciously discern the mapping, leading to an easily achievable adaptation strategy.

Since the study aimed to explore the task and null-space adaptation strategy of subjects, an intermediate mapping was constructed as:

$$\mathbf{A}' = \begin{bmatrix} mean\left(PC_1, PC_5\right) \\ mean\left(PC_2, PC_4\right) \end{bmatrix} \tag{6}$$

By combining two dominant PCs with two intermediate PCs, the resulting mapping should not be physiologically attainable without being too intuitive.

A screen-scaling matrix S was also employed to contain the cursor movement within the boundary of the screen. This was achieved by first calculating the $[x, y]$ range of the raw hand-cursor mapping output, and scaling relative to the screen dimensions, giving:

$$\mathbf{S} = \begin{bmatrix} \frac{W}{2{*}max(C_X)} & 0 \\ 0 & \frac{H}{2{*}max(C_Y)} \end{bmatrix} \tag{7}$$

Where W and H are the width and height of the screen respectively. The final mapping is then obtained as:

$$\mathbf{A} = \mathbf{A}'\mathbf{S} \tag{8}$$

4 Methods

4.1 Obtaining the inverse mapping

As outlined in eq. 5, during the cursor task the motor system develops an inverse mapping of the task structure, based on an estimate of the true forward mapping employed by the task program. To obtain this estimate, denoted B_{reg}, a linear regression was performed on the end-point (target reached) data for every block from each subject.

4.2 Predicting task strategy

It has been suggested that the motor system may seek to exploit task-redundancy by shifting motor variability to redundant dimensions in order to preserve task-relevant accuracy, formalized within the the framework of optimal feedback control[12]. Originally, the theory describes optimizing the control of a particular aspect of task performance by minimizing the temporal integral of a given cost function across a movement, however this can be reduced to optimization of a single time-step, at the end-point of each trial.

One such 'cost function' that holds immediate relevance to motor control is the minimisation of joint movement. Considered along with the requirement of the endpoint cursor position to achieve a specific location $\mathbf{P}$, this can be formalized as:

$$J\left(\mathbf{H}\right) = \lambda \mathbf{H}^T\mathbf{H} + \left(\mathbf{P} - \mathbf{AH}\right)^T\left(\mathbf{P} - \mathbf{AH}\right) \tag{9}$$

Here, the first term represents the sum-of-squares of joint movements, and the second penalizes the squared end-point accuracy. The λ term is a regularization coefficient allowing relaxation of the end-point accuracy in order to reduce overall cost, the minimisation of which with respect to $\mathbf{H}$ then giving:

$$\mathbf{H} = \left(\lambda\mathbf{I} + \mathbf{A}^T\mathbf{A}\right)^{-1}\mathbf{A}^T\mathbf{P} \tag{10}$$

Given that physically, the strategy penalizes total joint movement, it is reassuring to find that in the case of constrained optimisation, enforcing the end-point accuracy in the limit as $\lambda \to 0$, the M-P inverse solution is recovered as in eq. 5.

4.3 Extending the cost function towards natural statistics

This generalized framework can be conveniently adapted to accommodate any cost-function. While the hypothesis of minimum joint movement constitutes an intuitive prediction, it is possible that it may be overly simplistic in its assumptions.

Firstly, the model assumes that movement in each joint carries the same energetic or physiological cost. This assumption could easily be scrutinized by considering the illustrative case of an abduction of the thumb to the rotation of the pinky MCP joint. Even superficially, it would be difficult to argue that these carry the same cost, given the comparative sizes of the muscles controlling the movement.

Secondly, the model assumes independence of all joints, giving no consideration to their biomechanical relationships. It is clear that whereas moving the thumb and index finger independently is fundamental to performing a number of essential natural gestures, independent movement of the PIP and DIP joints of a finger is effectively impossible, given that they are physiologically coupled via a common tendon.

Thirdly, correlation between joints may arise synergistically, corresponding to a 'neural' cost whereby particular gestures may be favourable over others due simply to frequency of expression, encoded at some location or distributed within the motor system.

If it were truly the case that the brain seeks to develop optimal strategies for minimizing these three conditions, it would be expected that these strategies be captured in the subject's natural statistics.

A convenient way to do so is use the covariance matrix of the subjects' natural statistics to weight the joint movements. The condition can be easily used to extend the concept of the previous unbiased joint movement minimisation (B_{min}) model through:

$$J\left(\mathbf{H}\right) = \lambda \mathbf{H} \mathbf{\Phi}^{-1} \mathbf{H}^{T} + \left(\mathbf{P} - \mathbf{A}\mathbf{H}\right)^{T} \left(\mathbf{P} - \mathbf{A}\mathbf{H}\right) \tag{11}$$

Where the inverse of the covariance matrix $\mathbf{\Phi}$ is used. This method of incorporating the natural statistics is especially attractive, as it concisely incorporates the weighting of individual and compound movements. In the covariance matrix, the variances of individual joints are represented by the diagonal terms, however the off-diagonal terms represent the covariances $\sigma\left(h_i, h_j\right)$ between particular joint combinations. Eq. 11 can again be minimized to give:

$$\mathbf{H} = \left(\lambda \mathbf{\Phi}^{\mathbf{-1}} + \mathbf{A}^{T} \mathbf{A}\right)^{-1} \mathbf{A}^{T} \mathbf{P} = \mathbf{B}_{cov}\left(\lambda\right) \mathbf{P} \tag{12}$$

Here, setting the limit as $\lambda \to 0$ once again recovers the M-P pseudoinverse case, and so in this case the choice of λ must be considered to effectively trade off the two competing constraints. In the following analysis, its value was set by minimization of the sum-of-squares difference between the predicted and observed end-point positions.

Due to the small end-point error allowed by the task, subjects were given some flexibility to trade-off a proportion of accuracy in favour of minimizing the cost associated finger navigation. The choice of λ therefore reflects the amount of 'relaxation' employed by the subject.

Eq. 12also has a close relationship to the properties of the natural statistics. Assuming the distribution of joint movements to be normally distributed about their means, which are zero considering their resting-normalized positions, the probability of a particular joint configuration in articulation-space may be represented by a multi-dimensional Gaussian function:

$$P\left(\mathbf{H}\right) = \left(\frac{1}{\sqrt{2\pi}}\right)^{J} \cdot \left(\frac{1}{\prod_{j=1}^{J}\sigma_j}\right) \cdot \exp\left(-\frac{1}{2}\sum_{j=1}^{J}\left(\frac{h_j}{\sigma_j}\right)^2\right) = \frac{1}{\sqrt{\left(2\pi\right)^{J}\left|\mathbf{\Phi}\right|}} \cdot \exp\left(-\frac{1}{2}\mathbf{H}^T\mathbf{\Phi}^{-1}\mathbf{H}\right) \tag{13}$$

Where $\left|\mathbf{\Phi}\right| = det\left(\left|\mathbf{\Phi}\right|\right)$. Taking the log of which gives:

$$log\left(P\left(\mathbf{H}\right)\right) = \left[-\frac{J}{2} \cdot log\left(2\pi\right) - log\left(\left|\mathbf{\Phi}\right|\right)\right] - \frac{1}{2}\mathbf{H}^T\mathbf{\Phi}\mathbf{H} = \alpha - \frac{1}{2}\mathbf{H}^T\mathbf{\Phi}\mathbf{H} \tag{14}$$

Therefore, as α is constant for all joint configurations, the cost-function developed in eq. 12 is equivalent to penalising joint movements according to their negative log-probability in articulation space.

Numerically, the inverse of a covariance matrix can be computed more efficiently by taking advantage of its properties as a positive semi-definite matrix, where the spectral decomposition can be applied as:

$$\mathbf{\Phi} = \mathbf{U}\mathbf{\Lambda}\mathbf{U}^T \tag{15}$$

Where $\mathbf{\Lambda}$ is a diagonal matrix containing the eigenvalues of $\mathbf{\Phi}$. $\mathbf{U}$ is an orthonormal matrix, which has the property $\mathbf{U}^T = \mathbf{U}^{-1}$, such that the inverse of $\mathbf{\Phi}$ can then be calculated simply as:

$$\mathbf{\Phi}^{-1} = \mathbf{U}\mathbf{\Lambda}^{\mathbf{-1}}\mathbf{U}^T \tag{16}$$

Where the inverse of the diagonal matrix $\mathbf{\Lambda}^{-1}$ is simply a diagonal matrix containing the reciprocals of the eigenvalues.

5 Results and discussion

5.1 Comparing centre-out vs. Pinball trials

5.1.1 Trial type does not affect drift from the task-manifold

During the centre-out trials, the subject was forced to return to a constant resting position in the centre of the screen before attempting each new target. In the pinball trials, subjects were free to move from one target to the next without returning to the centre.

If the strategy were also dependent on the trajectory to a particular target rather than simply its position, the end-point joint variance might could be expected to be greater in the pinball than in the centre-out trials, due to trial-to-trial drift between task-planes as discussed in section 3. However, taking the average variance across all joints, subjects and targets for each block in fig. 8b shows no consistent difference in variance, suggesting that subjects adopted specific gestures for each target.

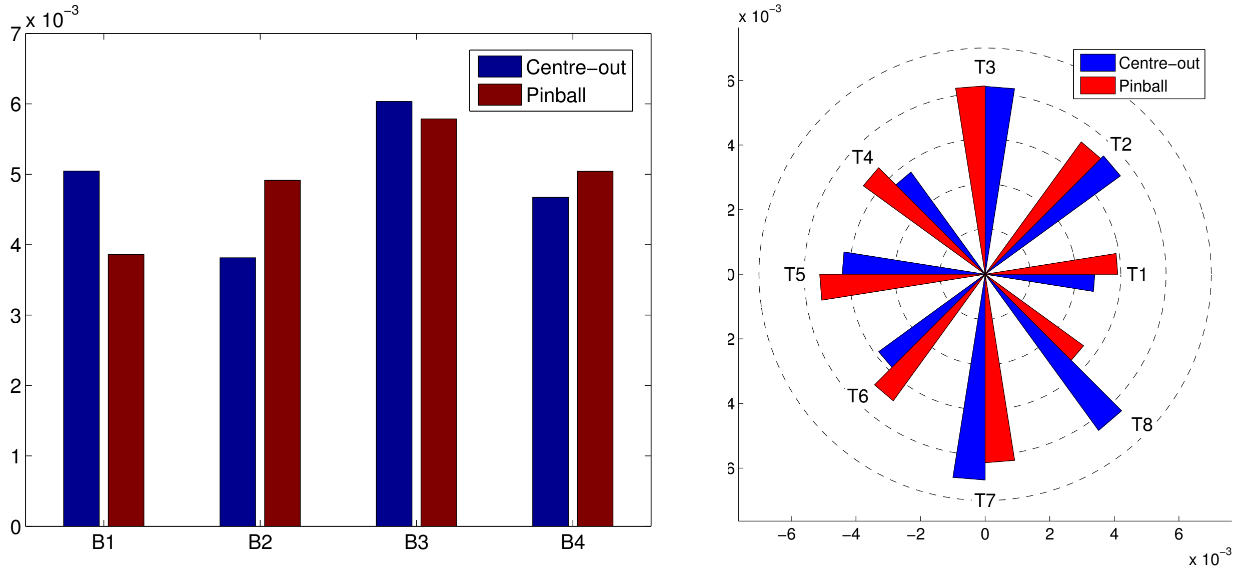

(a) Target and subject averaged variances across blocks

(b) Subject and block averaged variances across targets

Figure 8

5.1.2 Analyzing the effect of mapping on end-point variance

In the experiment, the x and y coordinates were governed by $mean\,(PC_1, PC_5)$ and $mean\,(PC_2, PC_4)$ respectively. These were chosen so as to investigate whether the choice of PCs affected the steady-state strategy adopted by subjects, the x-coordinate being a combination of a high and middling-frequency PC, and the y two middling-frequency PCs. Fig. 8b, displaying the average variance for each target position, shows targets with a greater y coordinate to have perceptibly higher variance, though the difference was not statistically significant.

Ingram and Wolpert found that the first two PCs accounted for $60.2 \pm 4.1\%$ of the variance, suggesting that lower ranked PCs correspond either to particularly rare well-defined gestures, or to a consistent amalgamation of intermediate gestures with no extreme joint flexions or extensions. In the latter case, the x-coordinate might not be distorted significantly by the 5th PC, whilst the y-coordinate, already corresponding to a weaker PC, would be distorted more significantly by the 4th PC. Under this assumption, movement in the x-coordinate would be controlled by a more natural sequence of gestures, making it easier relative to movement in the y-coordinate.

5.2 Comparing model predictions

5.2.1 The motor system learns a linear inverse geometric mapping of the task

Adopting consistent strategy during the tasks is equivalent to operating within a well-defined task-manifold in articulation space. Though the form of the inverse manifold formed by the motor system could take any form, the true task space is linear, consisting of J hyperplanes in $x - y - h_j$ space.

The inverse mapping estimated by the motor system was fitted by linear regression to the end-point data as outlined in section 4, an example of which is shown for one joint in fig. 9 for illustration. An intercept term was included to account for the possibility of drift from the resting position.

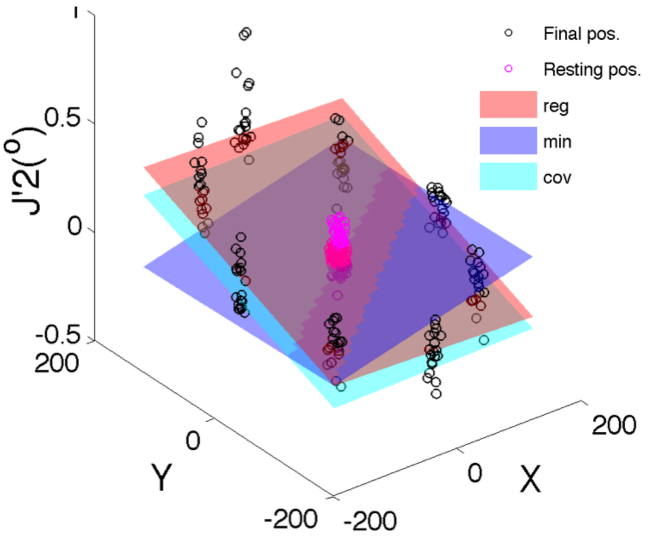

Figure 9: The B_{reg}, B_{min} and B_{cov} hyperplanes corresponding to one joint

The R^2 coefficients of the regression were averaged across subjects and blocks, and compared to those obtained from an ideal non-linear model, the latter simply equal to the means of the joint positions at

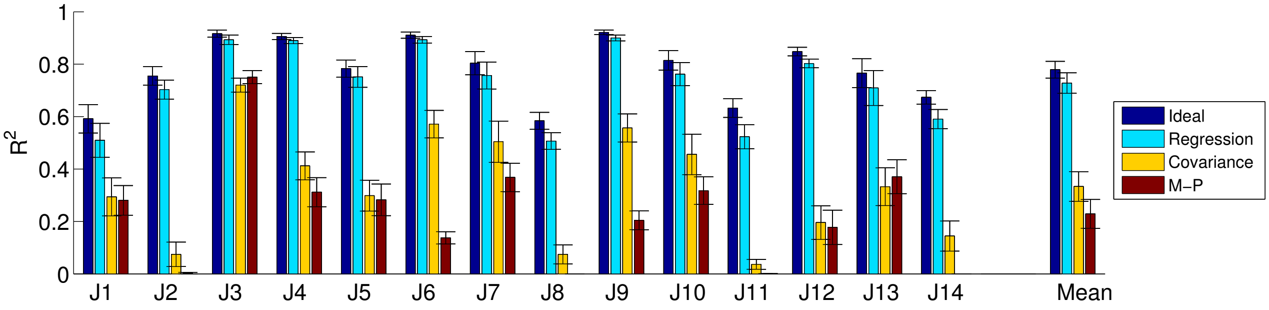

(a) CO

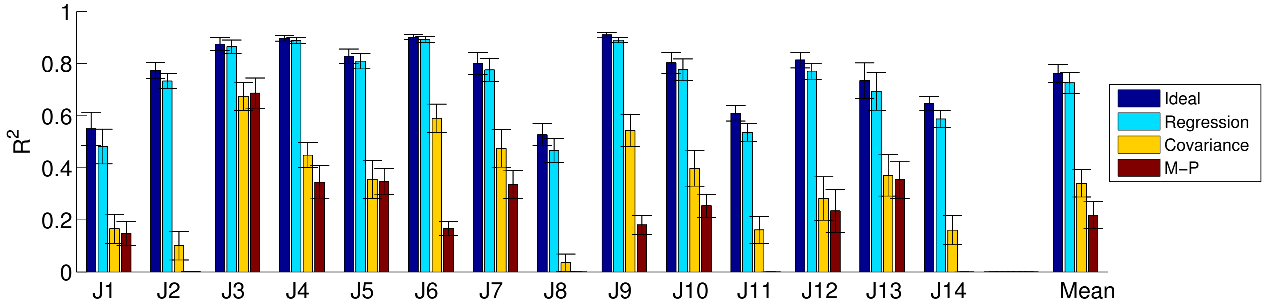

(b) PB

Figure 10: Subject and block averaged R^2 coefficients for contending models

each target, representing the best fit possible to the data. The results are shown in fig. 10, along with the joint averaged means.

Though both the ideal and regression models were significant over the null model (t-test, $p<0.01$) (single-parameter intercept), the ideal non-linear model was found not to be significant over the regression, showing that the internal task representation formed by the motor system is linear.

However, examining fig. 10 on a joint-by-joint basis shows that the effectiveness of the regression in explaining joint variance is in fact somewhat more volatile than suggested by the mean. More precisely, the R^2 decreases in magnitude for the MCPs (J4, J6, J9, J12), PIPs (J5, J7, J10, J13) and the inter-digit abductors (J8, J11, J14). The relationship between the fits is shown to be significantly correlated to the variance of the joints in fig. 11b.

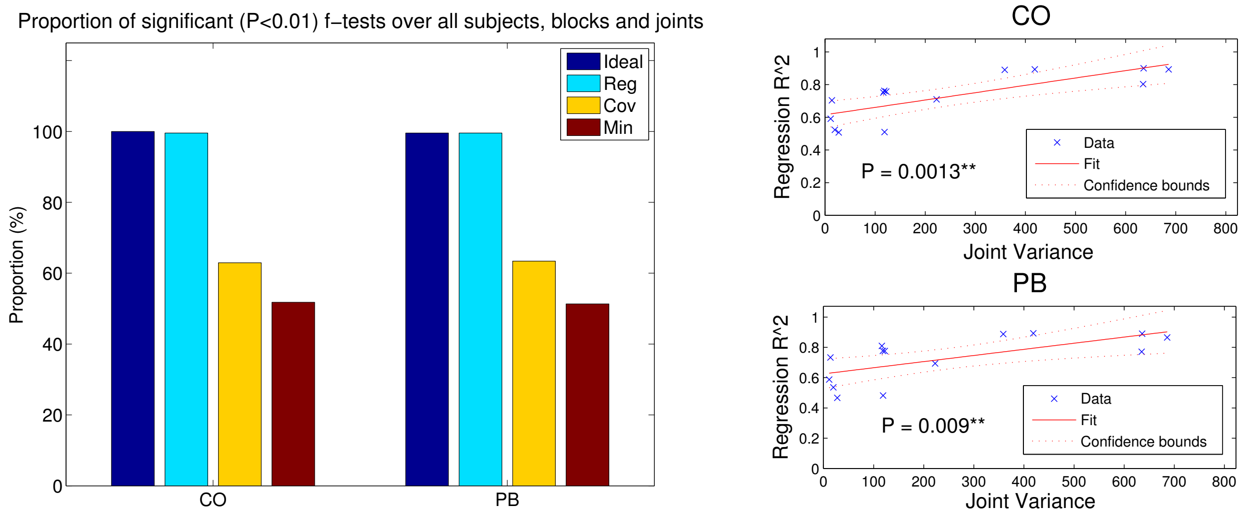

(a) Proportion of significant f-tests

(b) R^2 vs. Joint Variance (GSU)

Figure 11

This observation suggests that the motor system prioritizes reduction in motor variability according to joint variance, a strategy that would be consistent with reducing overall variability.

The proportions of significant R^2 values for each model (f-test, p<0.01) are shown in fig. 11a. On average, across subjects the ideal and regression models outperformed both the predictive models. However, the B_{cov} model is shown to be perceptibly better than the the simple B_{min} model, though more sample would be required to conclusively discern the significance of this result.

Though difficult to illustrate within the scope of this report, the B_{cov} and B_{min} models' average R^2 scores suffered as a result of inconsistency across subjects and joints. Where the regression and ideal models were guaranteed to align to some extent with the given data, a prediction by the B_{cov} or B_{min} models that misaligned the hyperplane gradient would produce an R^2 score of 0, significantly reducing the overall score.

In general, the predictions of both models were reasonable on joints where the regression and ideal model predictions were higher, and here the B_{cov} model was consistently superior to the B_{min}. These latter models also suffered from centering around the original resting position, from which significant deviation was actually observed over the course of blocks.

5.3 Comparing strategy across subjects

5.3.1 Motor variability is significantly lower in the task-space

As discussed in section 4, an important indication of structure learning in the task is a reduction of motor variance in the task-space comparative to the null-space, also consistent with optimal control theory. To investigate this, the end-point data was projected onto the two $J \times 1$ vectors describing the x and y components of the forward mapping matrix used by the program, and summed to give the task-space variance. The remainder after subtraction from the total variance, given by $tr\left(cov\left(\mathbf{H_{end}}\right)\right)$, gives the null-space variance. The results are shown in fig. 12.

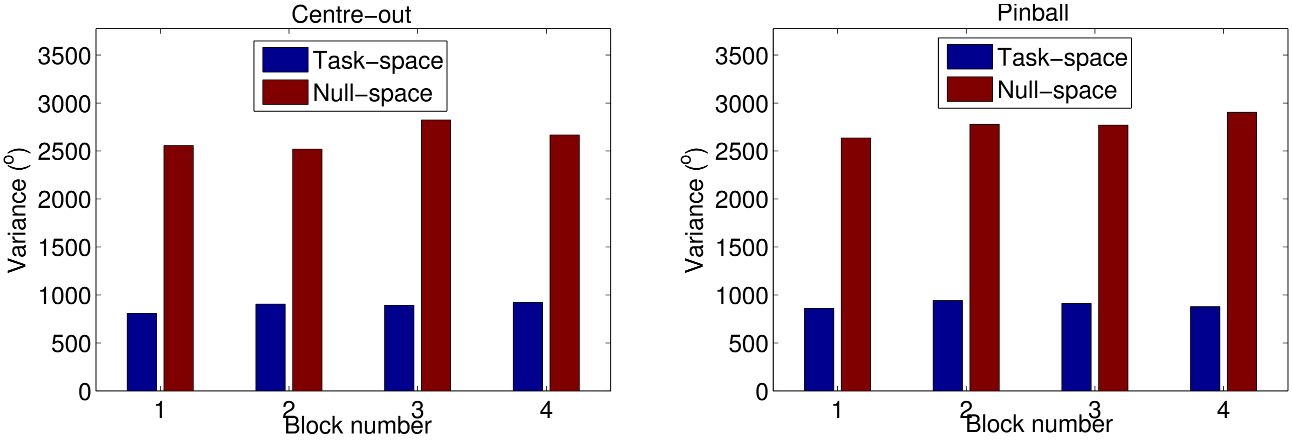

Figure 12: Task and null-space variance with block number

Firstly, the balance of task/null-space variance is almost identical in both trial-types, supporting the observations from section 5.1.1. Secondly, as expected, the average task-space variance over four blocks was significantly (t-test, $p<0.01$) lower than in the null-space.

However, principal components analysis of the end-point data shows that whilst the bulk of the variance cannot be accounted for by the true mapping components, a significant proportion of the variance is accounted for by relatively few principal components, shown in fig. 13.

Approximately 90% of variance is accounted for by the first two principal components, suggesting that whilst most of the movement within the task-space was controlled using two gestures, these gestures differed from the true gestures implemented in the forward mapping.

Whilst not alluding to a particular optimization scheme, the finding strongly suggests that the motor system adapted a consistent strategy that made concessions by incorporating movements in the null space, clearly optimizing a cost other than simple null-space movement.

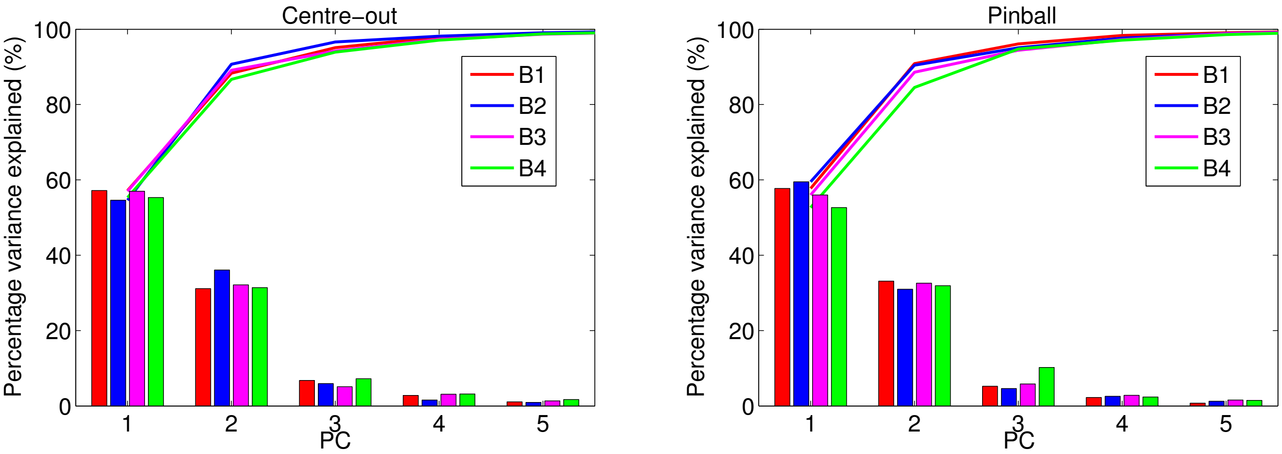

Figure 13: Cumulative variance explained by descending principal components

5.3.2 Subjects adopted significantly different strategies

Having established that the motor system adapts a consistent strategy within the task, analysis was conducted to discern whether these strategies were consistent across subjects.

In order to compare strategies across subjects, the average correlation distance between B_{reg} was calculated as the mean of all pairs of blocks within each subject, and compared to the average distance of all other combinations between subjects, shown in fig. 14. The analysis shows that subjects adopted significantly differing strategies across the task.

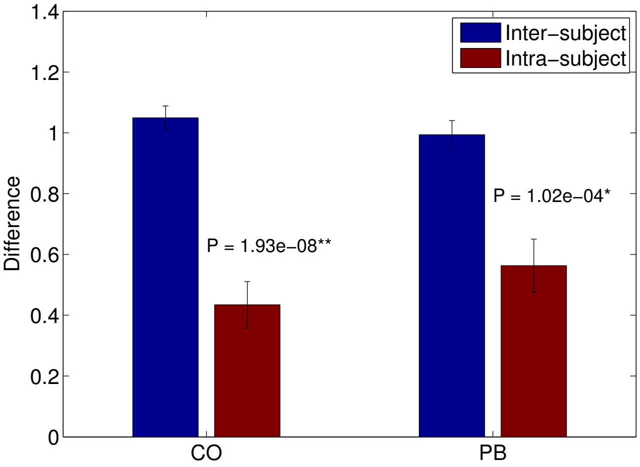

Figure 14: Average correlation distance, inter and intra-subject

6 Conclusions and further work

The current study investigated a number of themes in the context of motor learning in redundant control tasks. First, it was shown that during the experiment, subjects quickly learned to associate on-screen cursor positions with specific gestures required to achieve them in articulation space. Consequently, subjects did not show significant deviation from their chosen task-plane when presented with trials that could potentially expose trajectory, rather than simply position based strategies.

The finding is however not conclusive, and two further experiments could be conducted to further explore the finding. In future tasks, subjects should firstly be exposed explicitly either to the centre-out or pinball tasks, and secondly be tested on a generalization task with new target positions, to test the motor systems full representation of navigation within the task structure.

Secondly, it was found that the choice of mapping had a slight effect on the task-space variance in both x and y coordinates. Whilst not a particularly surprising finding in itself, it could be potentially exploited in further tasks to explore in more fundamental detail how learning is affected by the unfamiliarity of the forward mapping scheme.

Thirdly, the end-point data of subjects' performance was analyzed, showing little evidence that a non-linear model of the internal geometric mapping over a linear model. In order to discern whether the motor system interpreted a linear mapping in response to the given linear forward mapping, future experiments should investigate the implementation of non-linear mapping schemes.

Thirdly, two predictive models, B_{cov} and B_{min} were tested against observations of actual subject performance. A significant correlation was found between the consistency of strategy and individual joint variance. The B_{cov} model was shown to perform better than the B_{min} model, though further investigation is required to establish the significance of this result. More conclusive analysis would perhaps result from selective analysis of R^2 performance on a joint by joint basis, a subset (MCP, PIP) of which showed consistently less variance than others (abductors).

Lastly, it was demonstrated that subjects adopted significantly different strategies, though these strategies were influenced by common elements of the mapping scheme.

Appendix

Combining Covariance Matrices

Data from experimental trials was captured in the form of continuous monitoring of both cursor and joint positions at a rate of 10 fps. Consequently, to process the natural statistics of an entire block of trials would require the simultaneous loading into memory and concatenation of several of these large files. In order to circumvent the limited computing memory, the covariance matrix of each trial was computed separately and later combined to produce the total covariance matrix, where the combination method was devised as follows. Firstly, the covariance of two vectors x_i and x_j is defined as:

$$cov\left(x_i, x_j\right) = \frac{1}{N-1}\sum^{N} X_i.X_j = \frac{1}{N-1}\sum^{N}\left(x_i - \bar{x}_i\right).\left(x_j - \bar{x}_j\right) \tag{17}$$

Where $\bar{x}_i$ is the mean of the x_i vector. The covariance matrix is then described by:

$$Cov\left(\mathbf{M}_{O,P}\right) = \begin{bmatrix} \sum X_1.X_1 & \sum X_1.X_2 & ... & \sum X_1.X_P \\ \sum X_2.X_1 & \sum X_2.X_2 & ... & \sum X_2.X_P \\ ... & ... & ... & ... \\ \sum X_P.X_1 & \sum X_P.X_2 & ... & \sum X_P.X_P \end{bmatrix} \tag{18}$$

Where P is the number of variables and O the number of observations. Eq. 17 can be expanded in the case where the vectors x_i and x_j are split into two datasets as:

$$cov\left(x_i, x_j\right) = \frac{1}{N-1}\left\{\sum^{n_A}\left(x_{iA} - \bar{x}_i\right).\left(x_{jA} - \bar{x}_j\right) + \sum^{n_B}\left(x_{iB} - \bar{x}_i\right).\left(x_{jB} - \bar{x}_j\right)\right\} \tag{19}$$

$$= \begin{array}{l} \frac{1}{N-1}\left\{\sum^{n_A}\left(x_{iA} - \left(\frac{n_A\bar{x}_{iA}+n_B x_{\bar{i}B}}{n_A+n_B}\right)\right).\left(x_{jA} - \left(\frac{n_A\bar{x}_{iA}+n_B x_{\bar{i}B}}{n_A+n_B}\right)\right)\right\} \\ +\frac{1}{N-1}\left\{\sum^{n_B}\left(x_{iB} - \left(\frac{n_A\bar{x}_{jA}+n_B x_{\bar{j}B}}{n_A+n_B}\right)\right).\left(x_{jB} - \frac{n_A\bar{x}_{jA}+n_B x_{\bar{j}B}}{n_A+n_B}\right)\right\} \end{array} \tag{20}$$

$$= \frac{1}{N-1}\left\{\sum^{n_A}\left(\left(x_{iA} - \bar{x}_{iA}\right) - \left(\frac{n_A\bar{x}_{iA} + n_B x_{\bar{i}B}}{n_A + n_B} - x_{\bar{i}A}\right)\right).\left(\left(x_{jA} - x_{\bar{j}A}\right) - \left(\frac{n_A\bar{x}_{iA} + n_B x_{\bar{i}B}}{n_A + n_B} - x_{\bar{j}A}\right)\right)\right\} + \{...\} \tag{21}$$

$$= \frac{1}{N-1}\left\{\sum^{n_A}\left(X_{iA} + \frac{n_B}{N}\left(x_{\bar{i}A} - x_{\bar{i}B}\right)\right).\left(X_{jA} - \frac{n_B}{N}\left(x_{\bar{j}A} - x_{\bar{j}B}\right)\right)\right\} + \{...\} \tag{22}$$

$$= \frac{1}{N-1}\left\{\sum^{n_A}\left(X_{iA} + \frac{n_B}{N}\alpha_i\right).\left(X_{jA} - \frac{n_B}{N}\alpha_j\right)\right\} + \{...\} \tag{23}$$

$$= \frac{1}{N-1}\left\{\sum^{n_A} X_{iA}.X_{jA} + \sum^{n_A} X_{iA}\frac{n_B}{N}\alpha_j + \sum^{n_A} X_{jA}\frac{n_B}{N}\alpha_j + \sum^{n_A}\left(\frac{n_B}{N}\right)^2 \alpha_i\alpha_j\right\} + \{...\} \tag{24}$$

Since X represents the deviation vector (i.e with mean subtracted), its summation equals zero:

$$= \frac{1}{N-1}\left\{\sum^{n_A} X_{iA}.X_{jA} + \sum^{n_A}\left(\frac{n_B}{N}\right)^2 \alpha_i\alpha_j\right\} + \{...\} \tag{25}$$

The sum of the mean over n_A is equivalent to simply multiplying it by n_A as it's a scalar. Finally, we can recognise the first term as the covariance of the subset vector, reducing the expression to:

$$= \frac{1}{N-1}\left\{cov\left(x_{iA}, x_{jA}\right) * \left(n_A - 1\right) + \frac{n_A n_B^2}{N^2}\alpha_i\alpha_j\right\} + \{...\} \tag{26}$$

We can now combine elements of two covariance matrices using the following expression:

$$C_{ij} = C_{ijA}\left(\frac{n_A - 1}{N-1}\right) + C_{ijB}\left(\frac{n_B - 1}{N-1}\right) + \frac{n_A n_B^2 + n_B n_A^2}{N^2\left(N-1\right)} \tag{27}$$

$$C_{ij} = C_{ijA}\left(\frac{n_A - 1}{N-1}\right) + C_{ijB}\left(\frac{n_B - 1}{N-1}\right) + \frac{n_A n_B}{N\left(N-1\right)} \tag{28}$$

References

[1] Morasso P. (1981), 'Spatial control of arm movements'. Experimental Brain Research.

[2] Soechting JF, Lacquaniti F. (1981), 'Invariant characteristics of a pointing movement in man'. The Journal of Neuroscience.

[3] Flash T, Hogan N. (1985), 'The coordination of arm movements: An experimentally confirmed mathematical model'. The Journal of Neuroscience.

[4] Mussa-Ivaldi FA, Casadio M, Danziger ZC, Mosier KM, Scheift RA (2011), 'Sensory motor remapping of space in human-machine interfaces'. Prog. Brain Res.

[5] Shadmehr R, Mussa-Ivaldi FA. (1994), 'Adaptive representation of dynamics during learning of a motor task'. The Journal of Neuroscience.

[6] Lackner J, Dizio P. (1994), 'Rapid adaptation to Coriolis force perturbations of arm trajectory'. Journal of Neurophysiology.

[7] Dingwell JB, Mah CD, Mussa-Ivaldi FA. (2002), 'Manipulating objects with internal degrees of freedom: Evidence for model-based control'. Journal of Neurophysiology.

[8] Dingwell JB, Mah CD, Mussa-Ivaldi FA. (2004), 'An experimentally confirmed mathematical model for human control of a non-rigid object'. Journal of Neurophysiology.

[9] Mosier KM, Scheidt RA, Acosta S, Mussa-Ivaldi FA. (2005), 'Remapping hand movements in a novel geometrical environment'. Journal of Neurophysiology.

[10] Bernstein, N. (1967), 'The coordination and regulation of movement'.

[11] Latash M. (2000), 'There is no motor redundancy in human movements. There is motor abundance'. Motor Control.

[12] Todorov E, Jordan MI. (2002), 'Optimal feedback control as a theory of motor coordination'. Nature Neuroscience.

[13] Liu X, Scheidt R. (2008), 'Contributions of online visual feedback to the learning and generalization of novel finger coordination patterns'. Journal of Neurophysiology.

[14] Welch RB, Bridgeman B, Anand S, Browman KE. (1993), 'Alternating prism exposure causes dual adaptation and generalization to a novel displacement'. Perception and Psychophysics.

[15] Braun DA, Aertsen A, Wolpert DM, Mehring C. (2009), 'Motor task variation induces structural learning'. Current Biolog.

[16] Liu X, Mosier KM, Mussa-Ivaldi FA, Casadio M, Scheidt RA. (2011), 'Reorganization of finger coordination patterns during adaptation to rotation and scaling of a newly learned sensorimotor transformation'. Journal of Neurophysiology.

[17] Danziger Z, Fishbach A, Mussa-Ivaldi FA. (2009), 'Learning algorithms for human–machine interfaces'. IEEE Transactions on Biomedical Engineering.

[18] Braun DA, Mehring C, Wolpert DM (2010), 'Structural learning in action'. Behavioural Brain Research.

[19] Wolpert DM, Diedrichsen J, Flanagan JR (2011), 'Principles of sensorimotor learning'. Nature Reviews Neuroscience.

[20] Verstynen T, Sabes PN (2011), 'How each movement changes the next: an experimental and theoretical study of fast adaptive priors in reaching'. Journal of Neuroscience.

[21] Huang VS, Haith A, Mazzoni P, Krakauer, JW, (2011), 'Rethinking motor learning and savings in adaptation paradigms: model-free memory for successful actions combines with internal models'. Neuron.

[22] Ingram JN, Kording KP, Howard IS, Wolpert DM (2009), 'The statistics of natural hand movements'. Exp Brain Res.

[23] Gentner R, Classen J (2006), 'Modular Organization of Finger Movements by the Human Central Nervous System'. Neuron.

[24] Gentner R, Gorges S, Weise D, Kampe K, Buttman M, Classen J (2010), 'Encoding of Motor Skill in the Corticomuscular System of Musicians'. Current Biology.

[25] Overduin SA, d'Avella A, Carmena JM, Bizzi E (2012), 'Microstimulation Activates a Handful of Muscle Synergies'. Neuron.

[26] http://www.cyberglovesystems.com/

[27] Snedecor, George W. and Cochran, William G. (1989), 'Statistical Methods', Eighth Edition, Iowa State University Press.